

Microstructure-related relaxation and spin-wave linewidth in polycrystalline ferromagnetsU. Hoeppe^{1,2} and H. Benner¹¹*Institut für Festkörperphysik, TU Darmstadt, Germany*²*Advanced Ferrite Technology GmbH, Backnang, Germany*

(Received 4 May 2004; published 8 April 2005)

The theoretical approach of two-magnon scattering in polycrystalline ferrites by Sparks, Loudon, and Kittel [Phys. Rev. **122**, 791 (1961)] aiming at the microstructure-related relaxation of the uniform precession mode is extended to describe the relaxation of spin-wave modes. Within this framework we introduce a unified model that describes the influence of pores and microdomains on the relaxation of both the uniform precession and spin-wave modes. It is shown that the spin-wave linewidth does not only depend on the wave number—as assumed in conventional theory—but also on the propagation direction of the spin waves. This will, in particular, affect the damping of the critical modes at spin-wave instabilities, when probed in different experimental configurations. The effect of the number and size of pores as well as the influence of domain size and anisotropy is studied in detail, and as will be shown, this results in quite different parameter dependencies. Good qualitative and even quantitative agreement with previous experimental data is achieved without using any fit parameter.

DOI: 10.1103/PhysRevB.71.144403

PACS number(s): 75.50.Tt

I. INTRODUCTION

The present boom in the communication industry has raised the demand for specific microwave ferrite materials necessary to construct passive microwave devices, such as isolators or circulators. High-power applications (e.g., components for transmitters, accelerators or radars) require specific materials having low-loss properties in combination with a stable high-power performance. From the point of view of the underlying physical mechanisms these technical requirements may be considered as antagonistic, since they call for low dissipation of the uniform magnetization mode, but for high dissipation of critical spin-wave modes in order to prevent the occurrence of instabilities^{1,2} that could destroy the device. In conventional material design these two demands exclude each other. Increasing the spin-wave damping, e.g., by chemical doping would simultaneously increase the damping of the uniform magnetization. Vice versa, the use of ultrapure materials would guarantee low propagation losses, but also decrease the spin-wave damping and, consequently, the instability threshold.

The recent progress of micro- and nanotechnology has offered new ways to influence material properties by manipulating the microscopic structure and to tailor these properties by specific kinds of preparation. This can be a way out of the above dilemma and allow one to change the dissipation of the uniform magnetization and of the spin-wave modes independently of each other. It is well known that the size of grains and pores in polycrystalline ferrites can dramatically affect the observed linewidths of ferromagnetic resonance (FMR). Schlömann³ attributed the broadening of the FMR line to microscopic nonmagnetic comprisals (*pores*) and was able to give a reasonable quantitative explanation in terms of his *single-pore model*. Later he studied the effect of local anisotropy in randomly oriented microdomains (*grains*) and explained the inhomogeneous broadening of the FMR in terms of his *independent grain model*.⁴ The relaxation of the uniform mode by pores and surface pits was investigated by

Sparks^{5–7} and explained by Sparks, Loudon, and Kittel (SLK)⁸ to result from two-magnon scattering processes. Experimental results concerning the influence of grain size on the spin-wave linewidth were explained in a phenomenological way by the *transit time model* by Borghese,^{9,10} Patton,^{11–13} and Scotter.¹⁴

All these models could qualitatively explain part of the observed effects, but a quantitative agreement was generally lacking, and some of their detailed predictions clearly contradict the experimental findings. For example, the approach by SLK⁸ as well as the transit time model^{11,15} predicted a wave-number dependence of the spin-wave linewidth linear in k , which means a vanishing effect of pores and grains on long-wave modes. In contrast to that many experiments did show that the linewidth of long-wave modes, too, is markedly increased with increasing porosity or decreasing grain size. So, in practice, experimental data have been fitted to trial functions, such as $\Delta H_k = A + Bk$,¹⁶ where the striking increase of the parameter A with porosity remained unexplained.

The aim of this paper is to discuss a microstructure-induced relaxation mechanism that could account for both cases. We will show that an extension of the SLK theory can explain the relaxation of both the uniform mode and of spin waves with arbitrary wave vector \mathbf{k} . We demonstrate that the common restriction to *wave-number* dependencies turns out to be insufficient, and one has also to include the *direction* of wave propagation. This means that the spin-wave linewidth ΔH_k is no longer universal for a given k , but depends on the kind of experiment performed. One important consequence will be that the thresholds for different types of spin-wave instabilities (e.g., first- and second-order Suhl instability,¹ parallel pumping instability)² are no longer related to each other but have to be explained by independent values of ΔH_k , since the respective critical modes are propagating in different directions. Within the same framework we extend our model to include the influence of grain size and anisotropy on relaxation. Their effect is studied, in detail, and

turns out to result in parameter dependencies quite different from that of the pores. We compare our results to experimental data from the literature.

II. THEORY

A. Porosity

The model by Sparks, Loudon, and Kittel⁸ attributes the microstructure-induced relaxation of the uniform mode in polycrystalline material to a two-magnon scattering process at pores or surface pits. For simplicity SLK considered the scattering potential of a single spherical pore located in the center of a spherical sample. By means of Fermi's golden rule the resulting decay rate for the uniform mode was derived. The superposition of many of such scattering centers finally yields the linewidth of the ferromagnetic resonance (which is just the relaxation rate of the uniform mode in field units) as a function of the density and size of the scattering pores. In the following we shall extend this approach to the more general case of spin waves with arbitrary wave vectors \mathbf{k} .

The magnetization $\mathbf{M}(\mathbf{r})$ is defined by the local density of (dimensionless) spins \mathbf{S}_i , each of them carrying a magnetic moment 2μ , summed up over a unit volume V (as far as possible we follow the notation of the original paper)

$$\vec{M}(\vec{r}) \equiv \frac{2\mu}{V(\vec{r})} \sum_{i, \vec{r}_i \in V(\vec{r})} \vec{S}_i. \quad (1)$$

By means of the Holstein-Primakov transformation¹⁷ the spin operators \mathbf{S}_i are transformed into magnon operators b_μ^+ and b_μ . To this end the Hamiltonian of the spin system consisting of Zeeman, dipolar and exchange energy, is diagonalized to obtain the form of a harmonic oscillator, where the b_μ^+ and b_μ can be understood to represent creation and annihilation operators for spin waves. The magnetization $\mathbf{M}(\mathbf{r})$ is written in terms of such magnon operators, and up to second order in b_μ^+ , b_μ its components read

$$M^z(\vec{r}) = M_s - \frac{2\mu}{V} \sum_{\mu, \nu} [e^{i(\vec{k}_\mu - \vec{k}_\nu) \cdot \vec{r}} b_\mu b_\nu^+ + e^{-i(\vec{k}_\mu - \vec{k}_\nu) \cdot \vec{r}} b_\mu^+ b_\nu], \quad (2)$$

$$M^+(\vec{r}) = \sqrt{\frac{4\mu M_s}{V}} \sum_{\mu} e^{i\vec{k}_\mu \cdot \vec{r}} b_\mu. \quad (3)$$

M_s is the saturation magnetization, and \mathbf{k}_μ and \mathbf{k}_ν are the wave vectors of the spin waves involved in the scattering process.

A pore affects the propagating spin waves by means of its demagnetization field $\mathbf{H}_d(\mathbf{r})$. The standard recipe from electromagnetic field theory to obtain \mathbf{H}_d is to calculate the gradient of the *magnetostatic potential* $\Phi(\mathbf{r})$

$$\vec{H}_d(\vec{r}) = -\text{grad } \Phi(\vec{r}) \quad \text{where} \quad \Phi(\vec{r}) = \int_{\text{sample}} \frac{\text{div } \vec{M}(\vec{r}')}{|\vec{r} - \vec{r}'|} d^3 r'. \quad (4)$$

For further convenience we split the demagnetization field into two parts, $\mathbf{H}_d(\mathbf{r}) = \mathbf{H}_b(\mathbf{r}) + \mathbf{H}_{sw}(\mathbf{r})$, where \mathbf{H}_b denotes the part originating from the boundary conditions of the magnetization at the surface of the pore and \mathbf{H}_{sw} denotes the intrinsic demagnetization field of the spin waves. Now, expressing the magnetization $\mathbf{M}(\mathbf{r})$ in terms of magnon operators according to (2) and (3) and using spherical coordinates we obtain for the first part of $\Phi(\mathbf{r})$ arising from the surface of the pore

$$\begin{aligned} \Phi_b(\vec{r}) &= \frac{4}{3} \pi R^3 \sqrt{\frac{4\mu M_s}{V}} \frac{1}{2} [e^{i\varphi} b_0^+ - e^{-i\varphi} b_0] \frac{\sin \Theta}{r^2} \\ &\quad - \frac{4}{3} \pi R^3 M_s \frac{\cos \Theta}{r^2}, \end{aligned} \quad (5)$$

and the corresponding components of $\mathbf{H}_b(\mathbf{r})$ read

$$\begin{aligned} H_b^\Theta(\vec{r}) &= -\frac{4}{3} \pi R^3 \sqrt{\frac{\mu M_s \cos \Theta}{V}} \frac{1}{r^3} [b_0^+ e^{i\varphi} - b_0 e^{-i\varphi}] \\ &\quad - \frac{4}{3} \pi R^3 M_s \frac{\sin \Theta}{r^3}, \end{aligned} \quad (6a)$$

$$H_b^\varphi(\vec{r}) = -i \frac{4}{3} \pi R^3 \sqrt{\frac{\mu M_s}{V}} \frac{1}{r^3} [b_0^+ e^{i\varphi} + b_0 e^{-i\varphi}], \quad (6b)$$

$$\begin{aligned} H_b^r(\vec{r}) &= -\frac{8}{3} \pi R^3 \sqrt{\frac{\mu M_s \sin \Theta}{V}} \frac{1}{r^3} [b_0^+ e^{i\varphi} - b_0 e^{-i\varphi}] \\ &\quad - \frac{8}{3} \pi R^3 M_s \frac{\cos \Theta}{r^3}. \end{aligned} \quad (6c)$$

The demagnetization field $\mathbf{H}_{sw}(\mathbf{r})$ arising from intrinsic part of the spin waves can be obtained the same way. The calculation is more tedious but straightforward,¹⁸ and the relevant terms yield

$$\begin{aligned} H_{sw}^x(\vec{r}) &= \sum_{\mu, \nu} \frac{4\pi 2\mu}{K^2 V} K^x K^z [e^{i\vec{k} \cdot \vec{r}} b_\mu b_\nu^+ + e^{-i\vec{k} \cdot \vec{r}} b_\mu^+ b_\nu] \\ &\quad - \sum_{\mu} \frac{4\pi}{k_\mu^2} \sqrt{\frac{\mu M_s}{V}} k_\mu^x [(k_\mu^x - ik_\mu^y) e^{i\vec{k}_\mu \cdot \vec{r}} b_\mu \\ &\quad + (k_\mu^x + ik_\mu^y) e^{-i\vec{k}_\mu \cdot \vec{r}} b_\mu^+], \end{aligned} \quad (7a)$$

$$\begin{aligned} H_{sw}^y(\vec{r}) &= \sum_{\mu, \nu} \frac{4\pi 2\mu}{K^2 V} K^y K^z [e^{i\vec{k} \cdot \vec{r}} b_\mu b_\nu^+ + e^{-i\vec{k} \cdot \vec{r}} b_\mu^+ b_\nu] \\ &\quad - \sum_{\mu} \frac{4\pi}{k_\mu^2} \sqrt{\frac{\mu M_s}{V}} k_\mu^y [(k_\mu^x - ik_\mu^y) e^{i\vec{k}_\mu \cdot \vec{r}} b_\mu \\ &\quad + (k_\mu^x + ik_\mu^y) e^{-i\vec{k}_\mu \cdot \vec{r}} b_\mu^+], \end{aligned} \quad (7b)$$

$$\begin{aligned}
H_{sw}^c(\vec{r}) = & \sum_{\mu,\nu} \frac{4\pi 2\mu}{K^2} \frac{2\mu}{V} K^z K^z [e^{i\vec{k}\cdot\vec{r}} b_{\mu} b_{\nu}^+ + e^{-i\vec{k}\cdot\vec{r}} b_{\mu}^+ b_{\nu}] \\
& - \sum_{\mu} \frac{4\pi}{k_{\mu}^2} \sqrt{\frac{\mu M_S}{V}} k_{\mu}^z [(k_{\mu}^x - ik_{\mu}^y) e^{i\vec{k}_{\mu}\cdot\vec{r}} b_{\mu} \\
& + (k_{\mu}^x + ik_{\mu}^y) e^{-i\vec{k}_{\mu}\cdot\vec{r}} b_{\mu}^+], \quad (7c)
\end{aligned}$$

where \mathbf{K} is defined by

$$\vec{K} = \vec{k}_{\mu} - \vec{k}_{\nu}. \quad (7d)$$

With these ingredients we are ready to determine the scattering potential S^{pore} for a two-magnon scattering process that reflects the change of dipolar energy when introducing the pore from outside into a homogeneous sample

$$\begin{aligned}
S^{\text{pore}} = & -\frac{1}{2} \left[\int_{\text{Sample with pore}} \vec{M} \cdot \vec{H}_d d^3r \right. \\
& \left. - \int_{\text{Sample without pore}} \vec{M} \cdot \vec{H}_d d^3r \right]. \quad (8)
\end{aligned}$$

We emphasize that the scattering potential is given by the *change* of the dipolar energy inside the sample, and not by the total dipolar energy as proposed in the original paper.⁸ This ansatz will guarantee that we strictly separate the scattering by the pore from other processes which may already occur in the homogeneous material.

To make the evaluation of the integrals as simple as possible, we have already chosen spherical shapes for sample and pore and a concentric location. We profit from the high symmetry of such an arrangement by expanding the spatial phase factors $\exp(i\mathbf{k}\cdot\mathbf{r})$ into spherical harmonics. Taking advantage of their orthogonality relations the three-dimensional integrals can be solved exactly. Then the scattering potential S for spin-wave modes with arbitrary wave vectors \mathbf{k}_{μ} reads explicitly [since we only focus on two-magnon scattering processes, terms $\sim (b_{\nu}^+ b_{\mu}^+ + \text{c.c.})$ have been omitted]

$$\begin{aligned}
S^{\text{pore}} = & 2\pi\mu M_s \frac{V_{\text{pore}}}{V} \sum_{\nu,\mu} (12 \cos^2 \Theta_K - 8 + 3 \cos^2 \Theta_{k_{\mu}} \\
& + 3 \cos^2 \Theta_{k_{\nu}}) \frac{j_1(KR)}{KR} [b_{\nu} b_{\mu}^+ + b_{\nu}^+ b_{\mu}] \\
& + \alpha \sum_{\nu} [b_{\nu} b_0^+ + b_{\nu}^+ b_0], \quad (9)
\end{aligned}$$

while for the special case of the uniform mode ($\mathbf{k}_{\mu}=\mathbf{0}$) we get

$$\begin{aligned}
S^{\text{pore}} = & 12\pi\mu M_s \frac{V_{\text{pore}}}{V} [3 \cos^2(\Theta_{k_{\nu}}) - 1] \frac{j_1(k_{\nu}R)}{k_{\nu}R} \\
& \times \sum_{\nu} [b_{\nu} b_0^+ + b_{\nu}^+ b_0]. \quad (10)
\end{aligned}$$

Here V_{pore} is the volume of the pore and V the volume of the sample. The fraction V_{pore}/V is called the *porosity* of the sample. The *scattering vector* $\mathbf{K}=\mathbf{k}_{\mu}-\mathbf{k}_{\nu}$ is given by the difference between the wave vectors of the incident spin

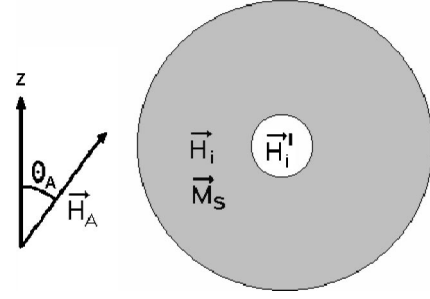


FIG. 1. Embedded grain model: Inside a grain the static internal field \mathbf{H}_i^1 differs from the mean value \mathbf{H}_i by the strength and direction of the effective anisotropy field \mathbf{H}_A .

wave \mathbf{k}_{μ} and of the scattered spin wave \mathbf{k}_{ν} , and Θ_K , $\Theta_{k_{\mu}}$, and $\Theta_{k_{\nu}}$ describe the corresponding directions. $j_1(x)$ denotes a spherical Bessel function of first order. For spin waves $\mathbf{k}_{\mu} > 0$ the α term in Eq. (9) turns out to become negligible in the following calculation because of the vanishing density of states for long-wave magnons within the spin-wave approximation. For the special case of the uniform mode the α term just compensates one part of the previous sum, so including it results in the less complicated form (10).

According to Fermi's golden rule the relaxation rate T_k^{-1} , which in magnetic field units means just the linewidth ΔH_k , for a magnon with wave vector $\mathbf{k}=\mathbf{k}_{\mu}$ is given by¹⁸

$$\gamma \Delta H_k = \frac{1}{T_k} = \sum_{\nu} \frac{2\pi}{\hbar} |\langle k_{\nu} | S^{\text{pore}} | k \rangle|^2 \delta(\hbar \omega_{k_{\nu}} - \hbar \omega_k). \quad (11)$$

Because of energy conservation required for the scattering process the spin wave \mathbf{k} with frequency ω_k is scattered only in spin waves \mathbf{k}_{ν} with frequencies $\omega_{k_{\nu}}=\omega_k$. By inserting (9) into (11), converting the sum into an integral, and taking account of the density of magnon states,

$$\rho(k_{\nu}) = \frac{V}{2\pi^2 \hbar} \frac{k_{\nu}^2}{\gamma 4\pi M_s \cos \Theta_{k_{\nu}}} \frac{\omega_k}{\gamma (Dk_{\nu}^2 + H_i)}, \quad (12)$$

we finally obtain the following expression for the linewidth of spin waves with arbitrary nonzero wave vectors \mathbf{k} :

$$\begin{aligned}
\Delta H_k^{\text{pore}} = & \frac{4\pi M_s V_{\text{pore}}}{12} R \omega_k \frac{1}{2\pi} \int_0^{2\pi} \int_{k_{\min}}^{k_{\max}} \frac{g(\Theta)}{\cos(\Theta_{k_2})} \left(\frac{j_1(KR)}{K} \right)^2 \\
& \times \frac{k_2^2}{\gamma (Dk_2^2 + H_i)} dk_2 d\varphi_2, \quad (13)
\end{aligned}$$

where \mathbf{k} is the wave vector of the relaxed spin-wave mode, \mathbf{k}_2 is the wave vector of the degenerate mode, and $\mathbf{K}=\mathbf{k}-\mathbf{k}_2$ their difference vector. Θ_k , Θ_{k_2} , and Θ_K are the corresponding polar angles with respect to the direction of the static field. φ_2 denotes the azimuthal angle between \mathbf{k} and \mathbf{k}_2 , and R is the radius of the pore. The angular dependent terms are defined by

$$g(\Theta) = (12 \cos^2 \Theta_K - 8 + 3 \cos^2 \Theta_k + 3 \cos^2 \Theta_{k_2})^2 \quad (14)$$

and

$$\cos \Theta_K = \frac{k_2 \cos \Theta_{k_2} - k \cos \Theta_k}{\sqrt{(k^2 + k_2^2) - 2kk_2(\cos \varphi_2 \sin \Theta_{k_2} \sin \Theta_k + \cos \Theta_{k_2} \cos \Theta_k)}}. \quad (15)$$

D is the spin-wave stiffness and H_i the internal static magnetic field. Finally, k_{\min} and k_{\max} have to be calculated as functions of frequency ω and static magnetic field H_i using the dispersion relation for spin waves.

For the particular case of uniform precession ($\mathbf{k}=0$) we reproduce the result obtained by SLK⁸

$$\begin{aligned} \Delta H_0^{\text{pore}} &= 3(4\pi M_s) \frac{V_{\text{pore}}}{V} R \omega_0 \\ &\times \int_{k_{\min}}^{k_{\max}} \frac{(3 \cos^2 \Theta_{k_2} - 1)^2}{\cos(\Theta_{k_2})} \frac{j_1^2(k_2 R)}{\gamma(Dk_2^2 + H_i)} dk_2. \end{aligned} \quad (16)$$

From (16) we can numerically calculate the resonance and off-resonance losses of the uniform mode, which will be of particular importance for material design. Because within most applications ferromagnetic materials—ferrites—are operated off resonance it is important to describe the influence of porosity in this regime. Here not only the total porosity V_{pore}/V but also the pore size R is very important, which is not the case on resonance.⁶ For example it can be shown from (16) that the bigger the pores the less is the influence on the off-resonance losses compared to the resonance linewidth. In experiment these losses are measured and described in terms of the so-called *effective linewidth*.¹⁵ From (13) we obtain the spin-wave linewidth for nonzero \mathbf{k} , which e.g., is necessary to determine the thresholds of spin-wave instabilities. Note that not only the porosity, i.e., the relative volume of the pores, but also the pore size is relevant, especially for $\mathbf{k} \neq 0$ modes. We emphasize that the linewidth of the spin waves is dramatically affected by their propagation direction, as will be further discussed in Sec. II C. The main advantage of our extended approach is that now the influence of porosity on the relaxation of the uniform mode as well as spin waves is treated within the same model. This provides us with more reliable grounds when designing materials with optimized microstructure.

B. Grain size and anisotropy

Schlömann⁴ has analyzed the influence of grain size and crystalline anisotropy on the relaxation of the uniform mode. Unfortunately his model is formally too complex to be extended to the general case of nonzero \mathbf{k} spin waves in a straightforward way. Here we develop a model describing the anisotropy-induced line broadening for nonzero k spin waves in terms of a two-magnon scattering process.

The basic idea is to replace the pore in our previous approach, Sec. II A, by a spherical “embedded” grain of radius R in the center of a spherical sample. The crystal orientation of this grain is well defined but arbitrary. Strength and direction of the crystalline anisotropy are described by an effective

anisotropy field \mathbf{H}_A , so that the effective static field inside the embedded grain is approximately given by $H_i' = H_i^z + H_A \cos \Theta_A$ (see Fig. 1). All other grains forming the polycrystalline sample are randomly oriented and are summarized in a mean field. Then the Hamiltonian for the two-magnon scattering process S^{grain} reflects the change of dipolar energy of the sample when “switching on” the anisotropy inside the embedded grain

$$\begin{aligned} S^{\text{grain}} &= -\frac{1}{2} \left[\int_{\text{sample with aniso.}} \vec{M} \cdot \vec{H}_i(\vec{r}) d^3r \right. \\ &\quad \left. - \int_{\text{sample without aniso.}} \vec{M} \cdot \vec{H}_i(\vec{r}) d^3r \right]. \end{aligned} \quad (17)$$

Focusing on two-magnon scattering contributions only, we can follow the formal derivation given in Sec. II A. By analogy with Eqs. (13) and (16) we obtain the linewidth contribution induced by grains for spin waves with arbitrary \mathbf{k}

$$\begin{aligned} \Delta H_k^{\text{grain}} &= 3 \frac{V_{\text{grain}}}{V} \frac{H_A^2 \cos^2 \Theta_A}{4\pi M_s} R \omega_k \frac{1}{2\pi} \\ &\times \int_0^{2\pi} \int_{k_{\min}}^{k_{\max}} \frac{j_1^2(KR)}{K^2 \cos \Theta_{k_2}} \frac{k_2^2}{\gamma(Dk_2^2 + H_i)} dk_2 d\varphi_2, \end{aligned} \quad (18)$$

and for the particular case of the uniform mode we get

$$\begin{aligned} \Delta H_0^{\text{grain}} &= 3 \frac{V_{\text{grain}}}{V} \frac{H_A^2 \cos^2 \Theta_A}{4\pi M_s} R \omega_0 \\ &\times \int_{k_{\min}}^{k_{\max}} \frac{j_1^2(k_2 R)}{\cos \Theta_{k_2} \gamma(Dk_2^2 + H_i)} dk_2. \end{aligned} \quad (19)$$

Here, Θ_A denotes the angle between the easy axis of the embedded grain and the magnetic field, R the grain radius, V_{grain} the grain volume and V again the volume of the sample. The crystalline anisotropy is randomly oriented, so when considering the contribution of all grains of the sample we have to average $\cos^2 \Theta_A$ over all orientations and replace it by its mean value $\frac{1}{2}$. In total we have $V_{\text{grain}} = V$ because each grain of the sample contributes to the scattering process, and the common prefactor in Eqs. (18) and (19) reduces to $1.5H_A^2 R \omega_{k,0} / 4\pi M_s$.

The Eqs. (18) and (19) describe the linewidth broadening resulting from the anisotropy-induced two-magnon scattering process. This way the two most important forms of microstructure, namely, porosity and grain size, can be treated *within a unified model*.

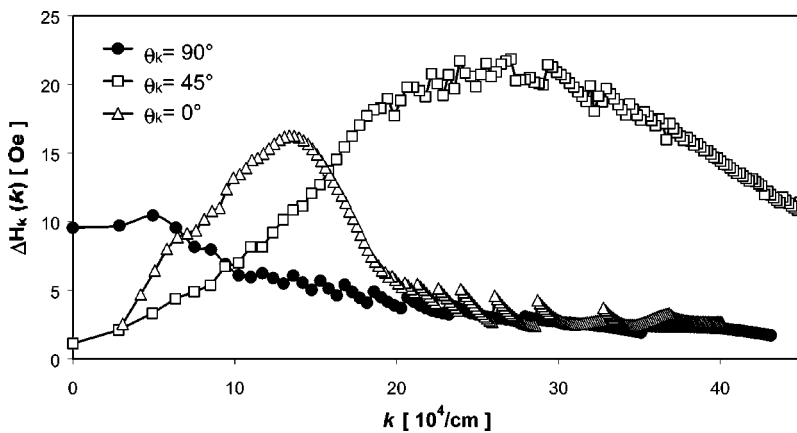


FIG. 2. Spin-wave linewidth $\Delta H_k(\mathbf{k})$ for $\omega_k = 4.5$ GHz calculated for polycrystalline YIG with 1% porosity and a pore size of $5 \mu\text{m}$.

C. k dependence of spin-wave linewidth

The k dependence of spin-wave linewidth ΔH_k has widely been discussed in the literature. It was found that for different experimental configurations, e.g., parallel pumping, first- and second-order Suhl instability, one had to use different fit parameters for ΔH_k to explain the corresponding data.^{11,16,19} Our model can explain these deviations in a straightforward way.

As a first approach let us neglect the angular dependence of ΔH_k , i.e., we assume that ΔH_k depends only on the wave number k . Then we find an approximate analytical solution for the integral in Eq. (13) as follows. For large R the function $j_1^2(KR)/(KR)^2$ is strongly peaked at $KR \approx 2$ and for sufficiently high values of the internal static field H_i we can replace the integrand by a δ function. Then Eq. (13) results in

$$\Delta H_k^{\text{pore}} \propto 4\pi M_S \frac{V_p}{V} \frac{\omega_k}{\gamma H_i} (k^2 R^2 + 4kR + 2). \quad (20)$$

We see that the spin-wave linewidth is no longer linear in k , as assumed in conventional theory and, in particular, in the SLK paper.⁸ Apart from the linear term there is a term proportional to k^2 and, even more important, a constant term, all of them reflecting two-magnon scattering processes induced by the pores. We emphasize that, even within such a rough approximation, we can for the first time explain the influence of microstructure on the relaxation of spin waves in the long-wave limit $k \rightarrow 0$.

In a qualitative way this simplified form shows already the main contributions, but it is still improved when including the full angular dependencies of Eqs. (13) and (18), which also turn out to be of major influence. Figure 2 shows the k dependence of the spin-wave linewidth ΔH_k calculated numerically from Eq. (13) for the propagation angles $\theta_k = 90^\circ, 45^\circ$ and 0° . (As will be discussed in Sec. III, according to standard theory^{1,2} these angles correspond to the critical, i.e., most unstable spin waves for the parallel pumping instability and for the first- and second-order Suhl instabilities.) Our simulations clearly demonstrate that the spin-wave linewidth is neither a simple constant nor a linear function of wave number k , but depends on both k and θ_k , in a more complicated way.

In order to get some intuitive understanding of these numerical results we have illustrated the scattering process in k space. Let us first consider the reason of the wave-number dependence. In the case of big pores the region in k space, which significantly contributes to the integral in Eq. (13) is a small sphere of radius $2/R$ [due to the term $j_1^2(KR)/(KR)^2$]. This sphere is centered close to the origin of k space when describing the scattering of long-wave modes [Fig. 3(a)]. For spin-waves with larger k , the small sphere is located farer away from the origin, which implies that for a given \mathbf{k} vector of direction θ_k all scattering contributions \mathbf{k}_2 have more or less the same direction [Fig. 3(b)] and the same amount. So, the angular dependent terms in the integral can be considered as constant, and the k_2 -dependent factor should directly re-

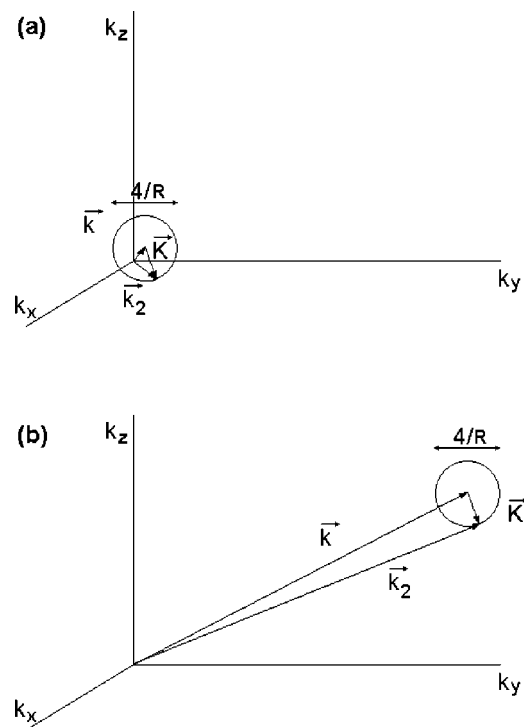


FIG. 3. Relevant region in k space for the scattering process in big pores. (a) For small wave numbers the small sphere of radius $2/R$ yields contributions from a large solid angle. (b) For large wave numbers only a small angle contributes significantly to the integral.

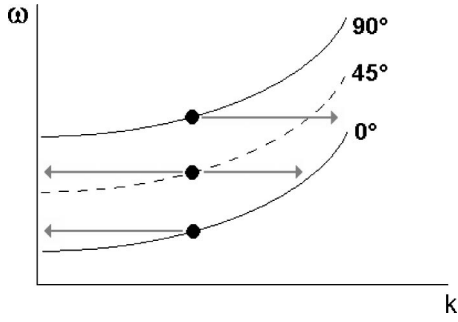


FIG. 4. Location of critical modes in the spin-wave band.

fect the k dependence of the spin-wave linewidth $\Delta H_k \sim k^2(Dk^2 + \omega)^{-1}$. In the large k limit $Dk^2 \gg \omega$ this factor, too, becomes constant. However, from the φ_2 -integration we get an extra weighting by $4/Rk$ reflecting the aperture of the small sphere. So in total, we obtain a dependence proportional to k for intermediate wave numbers [$K \ll k < (\omega/\gamma D)^{1/2}$], but proportional to $1/k$ for very large wave numbers. This is the reason for the increase of the spin-wave linewidth ΔH_k in Fig. 2 followed by a decrease after having passed a maximum.

The angular dependence of ΔH_k is somewhat more difficult to understand. It is plausible that the scattering geometry will be different when the wave vector of the incident spin wave is at the upper edge ($\theta_k=90^\circ$), in the middle ($\theta_k=45^\circ$), or at the lower edge ($\theta_k=0^\circ$) of the spin-wave manifold (Fig. 4). For big pores and large wave numbers k we have $\theta_k \approx \theta_{k2}$, and therefore, via the density of magnon states, we have a direct and pronounced influence of θ_k on the integrals of Eqs. (13) and (18).

In principle, the angular dependent factor $g(\theta)/\cos \theta_{k2}$ should explain the observed variation of linewidth taking $\theta_{k2} \approx \theta_k = 90^\circ, 45^\circ$, and 0° , respectively, while averaging θ over all possible directions. Qualitatively it is evident that, even when choosing the same sample and the same field and frequency parameters, we obtain different spin-wave linewidths for different experimental configurations, which is the consequence of the different propagation direction specific for the corresponding critical modes. This explains, e.g., the higher values of ΔH_k derived from the first-order Suhl instability ($\theta_k \approx 45^\circ$) compared to the parallel pumping case ($\theta_k \approx 90^\circ$). In fact, experimental data from the first-order Suhl instability and from the parallel pumping instability taken on the same set of samples did show a larger spin-wave linewidth in the first-order case.^{11,12,16}

Thus far only big scatterers were treated. For small scatterers (e.g., $R \leq 20$ nm), the relevant sphere in k space becomes very large and ΔH_k was found to be nearly *independent* of wave number k . For the same reason the angular dependence of ΔH_k vanishes and the scattering process becomes more isotropic, as recently suggested in Ref. 20. In fact, experiments have shown a *k-independent* increase of the spin-wave linewidth with decreasing grain size.¹² This behavior does not follow the embedded grain model but can be interpreted to result from many small scatterers located at the surface of the grains. Since the number of such small scatterers is expected to increase proportional to the ratio of

grain surface to volume (i.e., proportional to $1/R$), the experimental value of ΔH_k , which was found to be proportional to the inverse grain size, can be well explained by our model. Other explanations for this behavior are still missing.

III. APPLICATION TO HIGH-POWER PROPERTIES: THRESHOLD OF SPIN-WAVE INSTABILITY

Spin-wave instabilities are based on the resonant parametric excitation of spin waves induced by an external microwave field. The parametric mechanism is either based on the direct coupling of the spin waves with the microwave field component oscillating parallel to the static magnetic field (*parallel pumping*),² or indirectly by their dipolar coupling to the uniform mode pumped by a transverse microwave field (*first- and second-order Suhl instabilities*).¹ The efficiency of excitation depends on the damping of the modes to be excited, i.e., the spin-wave linewidth is the crucial property that determines the thresholds of these instabilities. Recall that the standard technique for evaluating ΔH_k is to measure the parallel pumping threshold.

Let us consider here the case of the first-order Suhl instability where the transverse pumped uniform mode excites a pair of spin waves at half the pumping frequency ($\omega = 2\omega_k$). For this configuration the critical microwave field h_c reads:¹

$$h_c = \left[\frac{\Delta H_k \omega_k}{\gamma 4\pi M_S \cos \Theta_k \sin \Theta_k} \frac{\sqrt{(\omega - \omega_0)^2 + (\gamma \Delta H_0/2)^2}}{(\gamma H_i + \gamma Dk^2 + \omega_k)} \right]_{\min}. \quad (21)$$

The threshold becomes lowest when simultaneously the resonance conditions for the uniform mode ($\omega = \omega_0$) can be satisfied, which is possible only for a limited frequency regime (the so-called coincidence regime). In any case, since the spin-wave linewidth ΔH_k for polycrystalline samples was found to be strongly k dependent, one has to minimize Eq. (21) on variation of both k and θ_k in order to find the mode with the lowest threshold. This critical mode is the first one to become unstable.

Figure 5 shows the numerical result based on the extended SLK theory and the embedded grain model. The minimization is carried out with respect to all possible k values of degenerate modes. The experimental data on YIG spheres were taken from Silber and Patton.¹⁶ The measured grain size a_0 was 30 and 5 μm , and the total porosity $p = V_p/V$ was 0.5% and 1.9%, respectively. We used these values in our simulation, and in addition we assumed an average pore size of 0.05 μm and an effective anisotropy field strength of 66 Oe. Our theoretical curve fits the experimental data quite well without using any fit parameters. A new and important result is that the increase of the threshold for higher magnetic fields H_i (corresponding to low k values) can qualitatively be well explained and shows even quantitatively reasonable coincidence. In particular, the observed increase of the minimum of the threshold curve with increasing porosity is well described. All previous models failed to explain such a behavior.

It is important to note that the k dependence of the spin-wave linewidth due to microstructure gives rise to an addi-

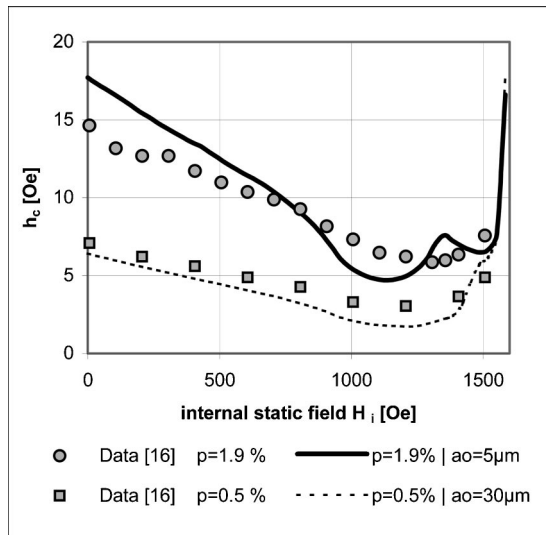


FIG. 5. Threshold of first-order Suhl instability for polycrystalline YIG with different porosities p of 0.5% and 1.9% and different average grain sizes a_0 of 5 and 30 μm , respectively. The dashed line shows calculated values for the dense sample and the solid line for the sample with higher porosity of 1.9%. The corresponding data are taken from Silber and Patton (Ref. 16).

tional frequency dependence of the threshold value. This was already observed by Green and Sandy¹⁹ in experiments on polycrystalline samples, but a connection with microstructure had not explicitly been proven. This frequency dependence is very important for technical application and has to be realized, when using the value of ΔH_k , determined from a standard parallel pumping experiment at 9 GHz, to calculate the threshold of, e.g., the first-order Suhl instability at, say, 3 GHz. The result could be wrong by a factor of 2.

IV. SUMMARY

The influence of the two main parameters of microstructure, porosity and grain size, on the relaxation of the uniform mode as well as spin-wave modes has been investigated within the framework of a unified model. By extending the SLK theory to account also for spin-wave modes with arbitrary \mathbf{k} , the effect of microstructure on the spin-wave linewidth ΔH_k is now well understood. In particular we were able to explain (i) the wave-number dependence of ΔH_k , (ii) the angular dependence of ΔH_k (concerning the direction of \mathbf{k}) which results in a drastic change of the linewidth for different experimental configurations, (iii) the importance of the size of pores and grains, (iv) the influence of the crystalline anisotropy, and (v) the effect of such linewidth properties on the threshold for spin-wave instabilities. Calculating the threshold of the first-order Suhl instability, we obtain realistic values for the threshold without using any fit parameters.

The detailed knowledge of the influence of microstructure on the relaxation of the uniform mode and of spin-wave modes brings us back to our starting problem: How to tailor low-loss ferrite materials with a stable high-power performance. The different effects of pores and grains on the linewidths of the uniform mode and of spin-wave modes can be the key for a possible design. For example, a small grain size seems to be optimal for a large spin-wave linewidth—and therefore also the instability threshold—and a relative small linewidth of the uniform mode. Moreover our calculations predict a strong dependence on frequency and direction of the relevant spin wave \mathbf{k} which also needs to be considered within the design process of such materials.

¹H. Suhl, *J. Phys. Chem. Solids* **1**, 209 (1957).

²E. Schlömann, J. J. Green, and U. Milano, *J. Appl. Phys.* **31**, 386 S (1960).

³E. Schlömann, *Proc. Conf. Magn. Magn. Mater.*, Boston (1956), p. 600.

⁴E. Schlömann, *Phys. Rev.* **182**, 632 (1969).

⁵M. Sparks, *Phys. Rev. Lett.* **8**, 54 (1962).

⁶M. Sparks, *Ferromagnetic-Relaxation Theory* (McGraw-Hill, New York, 1964).

⁷M. Sparks, *J. Appl. Phys.* **36**, 1570 (1965).

⁸M. Sparks, R. Loudon, and C. Kittel, *Phys. Rev.* **122**, 791 (1961).

⁹C. Borghese and R. Roveda, *J. Appl. Phys.* **40**, 4791 (1969).

¹⁰C. Borghese, *J. Phys. Colloq.* **38**, C1-261 (1977).

¹¹C. E. Patton, *J. Appl. Phys.* **41**, 1355 (1970).

¹²C. E. Patton, *J. Appl. Phys.* **41**, 1637 (1970).

¹³C. E. Patton, *IEEE Trans. Magn.* **8**, 433 (1972).

¹⁴D. G. Scotter, *J. Appl. Phys.* **42**, 4088 (1971).

¹⁵Q. H. F. Vrethen, *J. Appl. Phys.* **40**, 1849 (1969).

¹⁶L. M. Silber and C. E. Patton, *IEEE Trans. Magn.* **MAG-18**, 1630 (1982).

¹⁷See, e.g., R. M. White, *Quantum Theory of Magnetism* (Springer, Berlin, 1983).

¹⁸U. Hoeppe, Ph.D. thesis, Technische Universität Darmstadt, 2003, <http://elib.tu-darmstadt.de/diss/000332/Diss-Hoeppe-2003.pdf> (in German).

¹⁹J. J. Green and F. Sandy, *IEEE Trans. Microwave Theory Tech.*, Vol. **MTT-22**, 645 (1974).

²⁰M. J. Hurben and C. E. Patton, *J. Appl. Phys.* **83**, 4344 (1998).